Accepted Manuscript

STAT3 inhibition enhances CDN-induced STING signaling and antitumor immunity

Jianwen Pei, Yibo Zhang, Qinhong Luo, Wenlv Zheng, Wanxuan Li, Xin Zeng, Qinkai Li, Junmin Quan

PII: S0304-3835(19)30107-7

DOI: https://doi.org/10.1016/j.canlet.2019.02.029

Reference: CAN 14259

To appear in: *Cancer Letters*

Received Date: 26 November 2018

Revised Date: 8 February 2019

Accepted Date: 14 February 2019

Please cite this article as: J. Pei, Y. Zhang, Q. Luo, W. Zheng, W. Li, X. Zeng, Q. Li, J. Quan, STAT3 inhibition enhances CDN-induced STING signaling and antitumor immunity, *Cancer Letters*, https://doi.org/10.1016/j.canlet.2019.02.029.

STAT3 inhibition enhances CDN-induced STING signaling and antitumor immunity

Jianwen Pei[a,1], Yibo Zhang[a,1], Qinhong Luo[a], Wenlv Zheng[a], Wanxuan Li[a], Xin Zeng[a], Qinkai Li[a], Junmin Quan[a,*].

[a] State Key Laboratory of Chemical Oncogenomics, School of Chemical Biology and Biotechnology, Peking University Shenzhen Graduate School, Shenzhen, China.

[1] These authors contribute equally to this work.

* Correspondence should be addressed to J. Q. (quanjm@pku.edu.cn)

Abstract: Cyclic GMP-AMP synthase (cGAS)-stimulator of interferon genes (STING) pathway is a key regulator in innate immunity and has emerged as a promising drug target in cancer treatment, but the utility of this pathway in therapeutic development is complicated by its dichotomous roles in tumor development and immunity. The activation of the STING pathway and the induced antitumor immunity could be attenuated by the feedback activation of IL-6/STAT3 pathway. Here we reported that STAT3 inhibition significantly enhanced the intensity and duration of STING signaling induced by the STING agonist c-diAM$(PS)_2$. Such sensitization effect of STAT3 inhibition on STING signaling depended on STING rather than cGAS, which was mediated by simultaneously upregulating the positive modulators and downregulating the negative modulators of the STING pathway. Furthermore, the combination treatment with the STAT3 inhibitor and STING agonist markedly regressed tumor growth in syngeneic mice by increasing $CD8^+$ T cells and reducing regulatory T cells (Tregs) and myeloid-derived suppressor cells (MDSCs) in the tumor microenvironment. Our work provides a rationale for the combination of STAT3 inhibitors and STING agonists in cancer immunotherapy.

Keywords: STAT3 • cGAS-STING • Tumor microenvironment • Immunity • Immunotherapy

1. Introduction

Cyclic GMP-AMP synthase (cGAS)-stimulator of interferon genes (STING) signaling plays an important role in innate immunity by sensing cytosolic double-stranded DNA (dsDNA) [1-4]. cGAS recognizes self or pathogenic cytosolic DNA and subsequently catalyses the synthesis of cyclic GMP-AMP (cGAMP) from ATP and GTP [5]. cGAMP can bind to and activate STING [6, 7], leading to recruitment and phosphorylation of TBK1. Activated TBK1, in turn, activates interferon regulatory factor 3 (IRF3) and NF-κB, resulting in the production of type I IFNs and inflammatory cytokines, such as IL-6 and TNF-α [8]. During downstream paracrine or autocrine signaling, type I IFNs bind to cell surface receptors and initiate the activation of the JAK-STAT1/2 signaling pathway, regulating the transcription of hundreds of IFN-stimulated genes (ISGs) [9]. Similarly, IL-6 activates JAK-STAT3 signaling and initiates the transcriptional regulation of related genes [10].

The transient activation of the cGAS-STING signaling pathway is essential for host defense against pathogens, while sustained signaling is involved in autoimmune and inflammatory diseases and even inflammation-associated cancers. Thus, the cGAS-STING pathway needs to be tightly regulated [11-13]. Accumulating evidence has shown that cGAS-STING signaling participates in antitumor immunity, while defective cGAS-STING signaling is closely associated with the initiation and development of various tumors [14]. After tumor implantation or radiation therapy, tumor-derived DNA can access the cytosol of intratumoral dendritic cells (DCs), activating the cGAS-STING pathway to induce type I IFN production, promoting the maturation of DCs and triggering $CD8^+$ T cell priming to eliminate tumor cells [14, 15]. Several studies have also demonstrated the protective effects of the STING pathway and type I IFNs in glioma and colon cancer models [13, 16, 17]. Consistent with these studies, the STING ligand c-di-GMP

serves as an adjuvant in cancer vaccination to eliminate metastases in a breast cancer model [18]. In addition, the direct intratumorial delivery of cGAMP and its analogues in tumor-bearing immune competent mice substantially inhibits tumor growth and improves the survival of mice [19]. On the other hand, a deficiency in the STING pathway results in increased resistance to the development of 7,12-dimethylbenz[a]anthracene (DMBA)-induced skin tumors [20]. Moreover, the activation of the STING pathway in the tumor microenvironment may also facilitate immune evasion via the upregulation production of indoleamine 2,3-dioxygenase (IDO) and IL-10 production [21]. In addition to its roles in tumor development and immune evasion, cGAS-STING signaling is involved in tumor metastasis. Activation of STING in astrocytes by cGAMP transferred from tumor cells through gap junctions promotes the growth of metastatic brain cancer cells [20, 22]. Therefore, the therapeutic potential of exploiting cGAS-STING signaling requires a better understanding of its dichotomous roles in the tumor microenvironment.

cGAS-STING signaling promotes the production of IL-6 and the downstream activation of STAT3 [23], while less is known about the role of STAT3 in the STING pathway. Previous studies have shown that STAT3 negatively regulates STAT1-dependent inflammatory gene activation and type I IFN-mediated antiviral responses [24, 25]. In addition, STAT3 transduces signals from numerous oncogenic proteins and pathways to promote tumor cell proliferation and survival, and also to stimulate tumor angiogenesis and invasion [26, 27]. Recent studies have identified STAT3 as an important molecule that mediates tumor-induced immunosuppression, in which STAT3 regulates many genes that are crucial for immunosuppression, such as IL-10, TGFβ, IFN-β, IL-12 and CD80/86 [28-30]. Among these genes, IFN-β expression is increased by STAT3 inactivation through an unclear mechanism [28]. Given these findings, we are highly

intrigued by the question of whether STAT3 inhibition could contribute to STING signaling in anti-tumor immunity.

In this study, we demonstrated that the inhibition of the STAT3 pathway by a small-molecule inhibitor or siRNA markedly enhances STING signaling induced by the STING agonist c-diAM$(PS)_2$, although the STAT3 inhibitor does not induce STING signaling by itself. This sensitization effect on STING signaling primarily depends on multiple modulators of STING protein regulated by STAT3 inhibition. Furthermore, the combined STAT3 inhibitor and STING agonist treatment significantly enhanced tumor growth inhibition and the anti-tumor immune response in a 4T1 syngeneic mouse model compared with the single treatment. Our results provide new insights into the development of a novel combination therapy targeting both the STAT3 and STING pathways in cancer treatment.

2. Material and methods

2.1. Reagents, cells and antibodies

HJC0152 (CAS: 1420290-99-8) was purchased from Selleckchem (Houston, TX, USA) and dissolved in DMSO (Sigma-Aldrich, St Louis, MO, USA). c-diAM$(PS)_2$ was purchased from InvivoGen (San Diego, CA, USA, Catalogue #tlrl-nacda2r) and dissolved in endotoxin-free water. Both solutions were subsequently portioned into small aliquots and stored at -20°C. For the in vivo studies, the molecules were further diluted in buffer containing 2% DMSO, 10% HS15 and 0.9% NaCl. All other reagents used for buffers were purchased from Sigma-Aldrich. THP1 cells were purchased from SIBS (Shanghai, China). STING$^{-/-}$ THP1 cell line was a kind gift from Dr. Zhengfan Jiang (School of Life Science, Peking University, Beijing, China). Both THP1-Lucia^{TM} cells and THP1-Dual^{TM} KO-cGAS reporter cells were purchased from InvivoGen

(Catalogue #thpl-isg and #thpd-kocgas, respectively). All cells were cultured in RPMI1640 supplemented with 10% FBS and 0.1% Normocin (InvivoGen, Catalogue #ant-ar-1) at 37°C with 5% CO_2. 4T1 cells purchased from SIBS were stably transfected with genes encoding luciferase to generate 4T1-luc cells, which were cultured in DMEM containing 10% FBS. The antibodies used for immunblotting were as follows: anti-STAT3 (Cell Signaling, Danvers, MA, USA, Catalogue #9139), anti-phospho-STAT3 (Tyr705) (Cell Signaling, Catalogue #9145), anti-STAT1 (Abcam, Cambridge, UK, Catalogue #ab92506), anti-phospho-STAT1 (Tyr701) (Abcam, Catalogue #ab29045),anti-TBK1 (Cell Signaling, Catalogue #3504), anti-phospho-TBK1 (Ser172) (Cell Signaling, Catalogue #5483), anti-IRF3 (Cell Signaling, Catalogue #11904), anti-phospho-IRF3 (Ser386) (Abcam, Catalogue #ab76493), anti-STING (Cell Signaling, Catalogue #13647), anti-GAPDH (Cell Signaling, Catalogue #5174), and anti-cGAS (Cell Signaling, Catalogue #15102). The antibodies used for immunofluorescence were as follows: anti-TMEM173-Alexa Fluor® 488 (Abcam, Catalogue #ab198950), anti-ERGIC/p58-Cy3 conjugate (Sigma, Catalogue #E6782). The antibodies used for IHC-F were as follows: anti-mouse CD3e biotin (ebioscience, San Diego, CA, USA, Catalogue #13-0033-82), anti-mouse CD4 biotin (ebioscience, Catalogue #13-9766-82), anti-mouse CD8a biotin (ebioscience, Catalogue #13-0081-82), anti-mouse Foxp3 biotin (ebioscience, Catalogue #13-5773-82), anti-mouse Ly6G biotin (ebioscience, Catalogue #13-5931-82), and Streptavidin Alexa FluorTM 594 conjugate (Thermo Scientific, Waltham, MA, USA, Catalogue #S11227).

2.2. Real-time PCR

WT or $cGAS^{-/-}$ or $STING^{-/-}$ THP1 Cells were incubated with the drugs for specific time and w ere subsequently harvested in RNAiso Plus (TaKaRa, Dalian, Liaoning, China) for RNA isolatio

n according to the manufacturer's instructions. Next, the isolated RNA was transcribed using a T ransScript All-in-One First-Strand cDNA Synthesis Kit (TransGen Biotech, Beijing, China). To examine the mRNA levels, we utilized TB Green Fast qPCR Mix (Takara, Ostu, Shiga, Japan) a nd a CFX96 real-time PCR Detection System (Bio-Rad, Hercules, CA, USA). The expression da ta are expressed relative to the DMSO-treated cells and are normalized to the GAPDH C_t values. The sequences of the qPCR primers used in this study are as follows: 5'-GAACTTTGACATCC CTGAGGAGATT-3' and 5'-TGCGGCGTCCTCCTTCT-3' for *ifn* β, 5'-ATTTGCTGCCTTAT CTTTCTG-3' and 5'-CTTGATGGCCTTCGATTCTG-3' for *cxcl10*, 5'-CTTCGGTCCAGTTG CCTTCTC -3' and 5'-GCCTCTTTGCTGCTTTCACAC-3' for *il6*,5'-AGACTGAAGACTGAA CCTGAAGA-3' and 5'-GAACCCATTG-CGGCAAACATA-3' for *ifi16*, 5'-ATCCAGAGGAA TGTCACTCTCTT-3' and 5'-TGCGGCGTCCTCCTTCT-3' for *insig1*, 5'-CCTGCACGGACC CAAAGAA-3' and 5'-AGGGGTACAGTAGGCCAACAA-3' for *nlrc3*, and 5'-AAGGCTGTG GGCAAGGTCATC-3' and 5'-AGGTGGAGGAGTGGGTGTCG-3' for *gapdh*.

2.3. Immunoblotting

Indicated cells were incubated with the drugs for specific time and then harvested. Each sample was added with 150 μl SDS sample buffer（Sigma-Aldrich） and then boiled. After that, the samples were separated in 10% SDS-PAGE gels and subsequently transferred onto PVDF membranes (Millipore, Billerica, MA, USA). The membranes were blocked with 5% BSA in TBST (Tris-buffered saline with 0.1% Tween20) and then incubated with the indicated primary antibodies at 4°C overnight. The membranes were washed with TBST buffer for three times and then incubated with an HRP-conjugated anti-rabbit or anti-mouse IgG antibody (Cell Signaling) at room temperature for 1 hr. After the incubation and subsequent washing, bands were

developed using an FDbio Femto ECL kit (FDBio Science, Shenzhen, China) and then were exposed using MiniChemi (SAGECREATION, Beijing, China).

2.4. Enzyme-linked immunosorbent assay (ELISA)

Indicated cells were incubated with the drugs for specific time. Then cell culture supernatants were analysed by ELISAs for human CXCL10 (R&D Systems, Catalogue # DY814-05) levels, human IFNβ (R&D Systems, Catalogue # DY266-05) levels and human IL-6 (BD Biosciences, San Diego, CA, USA, Catalogue # 555220) according to the manufacturer's instructions.

2.5. RNA interference transfection

A total of 8×10^5 THP1 cells were seeded into each well of 6-well plates and were subsequently transfected with 350 nM of relevant STAT3-targeted siRNA from GenePharma (Shanghai, China) using Entranster-R4000 (Engreen Biosystem, Beijing, China). The siRNA target sequences were as follows: siRNA A: 5'-CCACTTTGGTGTTTCATAATT-3', B: 5'-GCAACAGATTGCCTGCATTTT-3', and negative control: 5'-TTCTCCGAACGTGTCACGTTT-3'. Lastly, 36 h after transfection, cells were treated as described.

2.6. Immunofluorescence

THP1 cells were differentiated by 320 nM PMA for 30 hr and then treated as described for indicated time. After that, the cells were fixed with cold absolute methanol and blocked with 1% BSA in PBST (PBS with 0.1% Tween20) for 1 hr. Finally, the cells were incubated with the indicated primary antibodies at 4°C overnight and further stained with Prolong Diamond

Antifade Mountant with DAPI (Invitrogen). Fluorescent images were acquired using a Nikon Confocal microscope (100× Objective).

2.7. In vivo tumor study

Animal studies were approved and overseen by the ethic committee of Laboratory Animal Center of Peking University Shenzhen Graduate School in accordance with the Policy on the Care, Welfare, and Treatment of Laboratory Animals. A total of 1×10^6 4T1-Luc cells were injected s.c. into 7- to 8-week-old Balb/C mice. When the tumor sizes reached approximately 100 mm^3, the mice were separated randomly into groups (n=6) and treated as described. Tumor sizes were measured every three days using callipers. Tumor volumes were calculated according to the following equation: (length × $width^2$)/2. In vivo tumor imaging was performed using an IVIS Spectrum Visualization System after the substrates were injected intraperitoneally into the mice.

2.8. IHC-F and fluorescence microscopy

Tumor tissues were fixed successively in 4% paraformaldehyde, 20% sucrose and 30% sucrose in phosphate-buffered saline and then were embedded in O.C.T. Compound (Sakura Finetek, Torrance, CA, USA, Catalogue #4583). The tissues were frozen in liquid nitrogen and then stored at -80°C. Upon usage, the frozen tissues were sectioned into 8-μm slices using a cryostat microtome (Leica, CM1950) and placed on positive charged slides. The slices then were allowed to air dry on a lab bench for a few minutes and blocked using normal goat serum at room temperature for 1 hr. Next, primary antibodies diluted in blocking buffer were added to each slice and incubated overnight at 4°C. Subsequently, the slices were incubated with a

fluorochrome-conjugated secondary antibody diluted in blocking buffer for 1 hr at room temperature in the dark. Finally, the slices were stained with Prolong Diamond Antifade Mountant with DAPI (Invitrogen) and covered with coverslips. Fluorescent images were acquired using an Olympus IX73 microscope (20× Objective) and were further processed and analysed using ImageJ.

2.9. RNA-Seq analysis

THP1 cells were incubated with the drugs for specific time. Then total RNA extraction, library preparation and RNA-Seq were carried out by BGI (Shenzhen, China). RNA-Seq was performed in triplicates. Differentially expressed genes were analysed with a DEGseq algorithm by BGI. The list of genes induced after stimulation was obtained by filtering the DEG list, and a heatmap of DEGs was generated with R.

2.10. Statistical analysis

All values were expressed as mean ± SD. Two tailed Student's t-test was performed for statistical comparison. Asterisk indicates that the values are significantly different (*, $P < 0.05$; **, $P < 0.01$; ***, $P < 0.001$).

3. Results

3.1. STAT3 inhibition enhances agonist-induced STING signaling

To evaluate the effect of STAT3 inhibition on STING signaling, we employed real-time quantitative PCR (qPCR) to examine mRNA levels of IFN-β and the downstream target gene CXCL10 in THP1 cells treated with the STAT3 inhibitor HJC0152 [31, 32] in the absence or

presence of the STING agonist c-diAM(PS)$_2$ [19, 33]. After 8 hr of treatment, HJC0152 significantly enhanced the expression level of IFN-β in a dose-dependent manner in the presence of c-diAM(PS)$_2$, which was not observed in the absence of c-diAM(PS)$_2$ (Fig. 1A). This result was further confirmed by that HJC0152 significantly enhanced the expression of IFN-β in the presence of increased amount of c-diAM(PS)$_2$ (Supplementary Fig. S1A), demonstrating that HJC0152 amplifies STING signaling induced by c-diAM(PS)$_2$ but does not induce the STING signaling by itself. Interestingly, in cells treated with HJC0152, no obvious amplification effect on the level of CXCL10 mRNA was observed in the presence of c-diAM(PS)$_2$ (Fig. 1B), while the amplification effect was observed after 12 hr of treatment (Supplementary Fig. S1B). This result may be due to interferon-stimulated genes expression being delayed compared with that of IFN-β [9], and the sensitization effect of HJC0152 on CXCL10 expression is displayed at a later time point. To test this hypothesis, we measured the expression of IFN-β and CXCL10 in THP1 cells treated with HJC0152, c-diAM(PS)$_2$, and HJC0152/c-diAM(PS)$_2$ at different time points. c-diAM(PS)$_2$ induced rapid IFN-β expression in a time-dependent manner that peaked at approximately 1 hr and then decreased gradually over the 24 hr treatment (Fig. 1C). As expected, the expression of CXCL10 in cells treated with c-diAM(PS)$_2$ peaked at approximately 8 hr and then decreased thereafter. Notably, the combined HJC0152 and c-diAM(PS)$_2$ treatment induced sustained IFN-β expression during the 24 hr treatment, and the expression of CXCL10 correspondingly peaked at approximately 12 hr and was significantly higher than that induced by c-diAM(PS)$_2$ alone at this time point (Fig. 1D). To further confirm the induction of IFN-β and CXCL10 by the combined HJC0152 and c-diAM(PS)$_2$ treatment, we used enzyme-linked immunosorbent assays (ELISA) to measure the amounts of IFN-β and CXCL10 protein

produced by THP1 cells. Consistent with the gene expression data, HJC0152 significantly enhanced the production of IFN-β and CXCL10 induced by c-diAM(PS)$_2$ (Fig. 1E, F).

Higher concentration of c-diAM(PS)$_2$ induced stronger STING signalling as reflected by increased mRNA level of IFN-β and its downstream genes such as CXCL10 (Supplementary Fig. S1A, B). On the other hand, 4 μg/ml or higher concentration of c-diAM(PS)$_2$ would cause significant cell death (Supplementary Fig. S1D). To avoid the potential side effect caused by the cell death, we therefore chose 2 μg/ml rather than 4 μg/ml c-diAM(PS)$_2$ in the following experiments.

Enhance STING signalling by higher concentration of c-diAM(PS)$_2$ also induced increased mRNA level of IL6 (Supplementary Fig. S1C, 2C), and the feedback activation of STAT3 (Supplementary Fig. S1E). STAT3 inhibitor HJC0152 markedly suppressed the feedback activation of STAT3 induced by c-diAM(PS)$_2$ (Supplementary Fig. S1E), and correspondingly decreased the accumulated secretion of IL6 (Supplementary Fig. S2D). On the other hand, combined HJC0152 with c-diAM(PS)$_2$ increased the activation of STAT1 due to the enhanced production of IFN-β (Supplementary Fig. S2A, B).

To verify the sensitization effect of STAT3 inhibition on STING signaling, we performed an immunoblot analysis of THP1 cells to characterize the STING-TBK1-IRF3 pathway upon treatment with HJC0152 and c-diAM(PS)$_2$. The results of this analysis demonstrated that HJC0152 markedly enhanced phosphorylation of TBK1 and IRF3 induced by c-diAM(PS)$_2$ in a time-dependent manner. Phosphorylation of TBK1 peaked at approximately 1 hr, and phosphorylation of IRF3 peaked at 4 hr, and sustained to approximately 12 hr, which is in agreement with TBK1 being the upstream kinase for IRF3 [8]. In contrast, the HJC0152 treatment did not enhance phosphorylation of TBK1 and IRF3 in the absence of c-diAM(PS)$_2$,

further demonstrating that the activation of the STING pathway is essential for the sensitization effect of STAT3 inhibition on STING signaling (Fig. 2A).

To exclude potential off-target effects of HJC0152, we evaluated the sensitization effect of direct knockdown of STAT3 on STING signaling induced by c-diAM(PS)$_2$. Similar to the HJC0152 treatment, knockdown of STAT3 via siRNA also greatly enhanced the expression of IFN-β and CXCL10 in THP-1 cells induced by c-diAM(PS)$_2$ (Fig. 2B, C). Evaluation of IRF3 phosphorylation further confirmed the enhancement of c-diAM(PS)$_2$-induced STING signaling by STAT3 knockdown (Fig. 2D).

3.2. The sensitization effect of STAT3 inhibition on STING signaling depends on STING but not cGAS

To determine the dependency of cGAS and STING for the sensitization effect of STAT3 inhibition on STING signaling, we measured the expression of IFN-β and CXCL10 in cGAS$^{-/-}$ and STING$^{-/-}$ THP1 cells treated with HJC0152 and c-diAM(PS)$_2$. As described above, HJC0152 significantly enhanced the expression of IFN-β and CXCL10 in the wildtype THP1 cells induced by c-diAM(PS)$_2$. Notably, the sensitization effect of HJC0152 was more prominent in cGAS$^{-/-}$ THP1 cells compared with the wildtype THP1 cells. In contrast to the wildtype and cGAS$^{-/-}$ THP1 cells, STING$^{-/-}$ THP1 cells completely abrogated the ability to respond to c-diAM(PS)$_2$ and also to HJC0152/c-diAM(PS)$_2$, suggesting that the sensitization effect of HJC0152 is associated with STING protein and the activation of STING signaling (Fig. 3A, B).

c-diAM(PS)$_2$ binds to STING protein and activates STING signaling, TBK1 is then activated by phosphorylation, leading to the recruitment and activation of IRF3. It is therefore not unexpected that c-diAM(PS)$_2$ treatment results in defection in the induction of phosphorylation

of TBK1 and IRF3 in STING$^{-/-}$ THP1 cells. The similar defection of the combined HJC0152 and c-diAM(PS)$_2$ treatment further confirmed that the sensitization effect of HJC0152 definitely depends on STING protein (Fig. 3C, D). On the other hand, the enhanced sensitization effect of HJC0152 on STING signaling in cGAS$^{-/-}$ THP1 cells was also demonstrated by the immunoblotting analysis, reflected by the increased phosphorylation of TBK1 and IRF3 in cGAS$^{-/-}$ THP1 cells treated by HJC0152/c-diAM(PS)$_2$ (Fig. 3C). The increased production of IFN-β and CXCL10 in cGAS$^{-/-}$ THP1 cells was confirmed by ELISA (Fig. 3D).

To further validate these observations, we used qPCR to examine mRNA levels of IFN-β and CXCL10 in cGAS$^{-/-}$ THP1 cells upon the combined HJC0152 and c-diAM(PS)$_2$ treatment over a 24-hr time course. Compared with the wildtype THP1 cells, the combined HJC0152 and c-diAM(PS)$_2$ treatment induced more rapid, robust and sustained expression of IFN-β and CXCL10 in cGAS$^{-/-}$ THP1 cells (Supplementary Fig. S3A, B). Correspondingly, the enhanced phosphorylation of TBK1 and IRF3 were detected at 1 hr and 4 hr, respectively, and both sustained to 24 hr (Supplementary Fig. S3C). Furthermore, the enhanced sensitization effect of STAT3 inhibition on STING signaling was also observed in PMA-differentiated THP-1 macrophages, which has significantly higher IFN-β and CXCL10 expression as compared to undifferentiated THP-1 cells (Supplementary Fig. S4). The translocation of STING from ER to ERGIC (ER-Golgi intermediate compartment) is critical for STING activation [1, 34]. We observed more profound perinuclear punctate structures in PMA-differentiated THP-1 macrophages treated with combined HJC0152 and c-diAM(PS)2 compared with that treated with either HJC0152 or c-diAM(PS)2, in which STING colocalized with the ERGIC markers (Fig. 4A, B).

3.3 STAT3 inhibition enhances agonist-induced STING signaling via transcriptional regulations

STING signaling can be regulated by multiple mechanisms such as protein degradation [35, 36], trafficking [35, 37-41], and associations [42-44]. To understand the mechanism underlying the sensitization effect of STAT3 inhibition on STING signaling induced by c-diAM$(PS)_2$, we evaluated RNA-Seq gene expression profiles in THP1 cells treated with HJC0152, c-diAM$(PS)_2$, and HJC0152/c-diAM$(PS)_2$ for 12 hr. Consistent with the results described above, the expression of IFN-β and numerous interferon-stimulated genes, including CXCL10, OAS family genes, and IFI family genes, was markedly upregulated by the combined HJC0152 and c-diAM$(PS)_2$ treatment compared with that observed in cells treated with HJC0152 or c-diAM$(PS)_2$ alone (Fig. 5A, B). Gene Ontology analysis further revealed that the top enriched genes are involved in type I interferon signaling pathway (Supplementary Fig. S5).

Both the HJC0152 and HJC0152/c-diAM$(PS)_2$ treatments downregulated the expression of cell proliferation genes such as MYC, CCND1, and BCL2, which is attributable to the STAT3 inhibition caused by HJC0152. Furthermore, some other genes suppressed by STAT3, such as STAT1, IRF7, and IRF9 [45, 46], were upregulated by the HJC0152 and HJC0152/c-diAM$(PS)_2$ treatments (Fig. 5A), which may provide positive feedback to the type I IFN signaling pathway.

Interferon-gamma inducible factor 16 (IFI16) has been proposed to activate STING signaling by sensing cytosolic DNA directly or in cooperation with cGAS [43]. Furthermore, IFI16 also facilitates the recruitment and activation of TBK1 in the STING complex [47]. To validate the enhanced expression of IFI16 in RNA-Seq analysis (Fig. 5A, B), we further determined the expression of IFI16 by qPCR (Supplementary Fig. S6). The single treatment of either HJC0152 or c-diAM$(PS)_2$ had a modest effect on the expression of IFI16, while the combined HJC0152 and c-diAM$(PS)_2$ treatment dramatically enhanced the expression of IFI16, which might partially

account for the sensitization effect of STAT3 inhibition on STING signaling induced by c-diAM(PS)$_2$. Furthermore, both RNAseq and qPCR analysis also demonstrated that HJC0152 or HJC0152/c-diAM(PS)$_2$ treatment significantly upregulated the expression of insulin-induced gene 1 (INSIG1) (Fig. 5A, B, Supplementary Fig. S6), an ER protein that facilitates the ubiquitination of STING and its association with TBK1 [35]. On the other hand, STAT3 inhibition by HJC0152 downregulated the expression of NLRC3 (Fig. 5A, B, Supplementary Fig. S6), a caspase activating and recruitment domain (CARD)-containing NLR that has been shown to directly bind to STING and impair its proper trafficking to perinuclear and punctuated region [48]. These results demonstrated that STAT3 inhibition enhances the STING signaling induced by c-diAM(PS)$_2$ through simultaneously upregulating the positive modulators and downregulating the negative modulator of STING signaling pathway.

3.4 STAT3 inhibition enhances STING-mediated anti-tumor immunity in vivo

STAT3 is a key molecular hub of tumorigenesis and tumor-mediated immune suppression [49, 50], while STING is essential for innate immune responses and $CD8^+$ T cell priming in the tumor microenvironment. Given the sensitization effect of STAT3 inhibition on STING signaling induced by the STING agonist, we examined the antitumor effect of the combination of HJC0152 and c-diAM(PS)$_2$. 4T1-Luc murine breast cancer cells were subcutaneously transplanted into immunocompetent BALB/c mice. When tumor volumes reached approximately 100 mm^3, animals received three intratumoral (i.t.) doses of HJC0152 (30 μg), c-diAM(PS)$_2$ (10 μg), or HJC0152/c-diAM(PS)$_2$ (30 μg/10 μg) over a one-week period. While the single treatment of either HJC0152 or c-diAM(PS)$_2$ had no effect or a modest inhibitory effect on tumor growth (-15.6% and 36.3% reduction for HJC0152 and c-diAM(PS)$_2$, respectively), the combined

HJC0152 and c-diAM$(PS)_2$ treatment significantly inhibited tumor growth (74.4% reduction; combination *vs.* vehicle: $p < 0.001$; combination *vs.* HJC0152: $p < 0.001$; and combination *vs.* c-diAM$(PS)_2$: $p < 0.01$) (Fig. 6A and Supplementary Fig. 6). More strikingly, the combined HJC0152 and c-diAM$(PS)_2$ treatment induced tumor regression over two weeks in 4 out of 6 (66.7%) mice, and over four weeks (the entire experimental period) in 1 out of 6 (16.7%) mice (Fig. 6C), highlighting that the combined HJC0152 and c-diAM$(PS)_2$ treatment has a lasting antitumor effect. This result was further confirmed by the appearance and weight of excised tumors (Fig. 6D, E). In addition, no significant body weight loss was observed during the experimental period for all treatments, including the control group (Fig. 6B), suggesting that the effective i.t. dose of the combined HJC0152 and c-diAM$(PS)_2$ treatment did not induce a severe toxic effect.

To evaluate the effects of HJC0152, c-diAM$(PS)_2$, and their combination on the immune response in the tumor microenvironment, we characterized the tumor-infiltrating immune cells in tumor tissues by immunohistochemistry (IHC). Using CD3e as a pan T-cell marker, we observed a modest increase in the number of $CD3e^+$ T cells in response to the single drug treatment compared to the vehicle treatment, while the combined drug treatment did not induce a significant increase in the number of $CD3e^+$ T cells compared to either single drug treatment (Supplementary Fig. 7 and Fig. 7C). Notably, the combined treatment caused a marked decreased in the number of $CD4^+$ T cells, especially $Foxp3^+$ T cells (Tregs) (Fig. 7C and Supplementary Fig. 8, 9), while it dramatically increased the number of $CD8^+$ T cells (CTLs) in tumor tissues compared to the other treatments (Fig. 7A, C). Furthermore, the combined treatment significantly decreased the accumulation of $Ly6G^+$ myeloid-derived suppressor cells (MDSCs) (Fig. 7B, C). These results demonstrated that the combined treatment profoundly

reduced the level of immune suppressive Tregs and MDSCs, and greatly induced the accumulation of cytotoxic $CD8^+$ T cells in the tumor microenvironment. We noted that the STING agonist c-diAM$(PS)_2$ induced substantial antitumor immune response by itself, and the STAT3 inhibitor HJC0152 further significantly enhanced this effect (Fig. 7C).

4. Discussion

In this study, we demonstrated that STAT3 inhibition by a small-molecule inhibitor HJC0152 or siRNA dramatically enhanced STING signaling induced by the STING agonist c-diAM$(PS)_2$. The observed enhancement was reflected in both the intensity and duration of STING signaling. The treatment of cells with 2 μg/ml c-diAM$(PS)_2$ alone induced weak IFN-β expression that peaked at approximately 1 hr before decreasing, while HJC0152 significantly amplified STING signaling induced by c-diAM$(PS)_2$ and sustained the signal for a longer period of time. This sensitization effect was dependent on STING but not cGAS, although the sensitization effect was more profound in $cGAS^{-/-}$ THP1 cells. Previously, STAT3 has been shown to attenuate type I IFN signaling in myeloid cells by sequestering STAT1 and suppressing the formation of DNA-binding STAT1 homodimers [25]. Moreover, STAT3 negatively regulates type I IFN signaling pathway by inhibiting the expression of STAT1, IRF7, and IRF9 [46]. However, there is currently little evidence describing how STAT3 inhibition increases IFN-β production through the STING pathway.

The STING pathway is regulated by multiple layers of mechanisms [51, 52]. Our data here indicated that the observed sensitization effect depends on STING rather than cGAS, suggesting that STAT3 inhibition regulates the downstream events of STING activation initiated by the CDN ligand (Fig. 3). Upon binding with agonists such as cGAMP, STING translocates from the

ER to an ER-Golgi intermediate compartment and to the Golgi apparatus, where STING recruits and activates TBK1, which subsequently phosphorylates IRF3 and activates the downstream type I IFN pathway [1]. During this process, IFI16 serves as a bridge that mediates the interaction between STING and TBK1 [47], INSIG1 also facilitates the association of STING with TBK1 through ubiquitination of STING [53], whereas NLRC3 impairs the proper trafficking of STING and the interaction between STING and TBK1 [48]. In the current study, we demonstrated that HJC0152 increases the expression of INSIG1 and decreases the expression of NLRC3. Moreover, HJC0152 synergizes with c-diAM$(PS)_2$ to upregulate the expression of IFI16. These results are consistent with the results of an immunoblot assay in which HJC0152 treatment was observed to enhance the phosphorylation of TBK1 and IRF3 induced by c-diAM$(PS)_2$. Furthermore, although IFI16 cooperates with cGAS in STING signaling, cGAS knockout would release more IFI16 to facilitate agonist-mediated recruitment of TBK1 to STING [43, 47], which may account for the enhanced sensitization effect of HJC0152 observed in $cGAS^{-/-}$ THP1 cells (Fig. 3, Supplementary Fig. S3A, B). In consistent with this hypothesis, the previous study has shown that PMA-stimulated differentiation dramatically decreased the level of cGAS while significantly enhanced the level of IFI16 in THP-1 cells, and the expression of IFI16 correlates with the ability of cells to induce IFN-β expression in response to *L. monocytogenes* infection[54]. Furthermore, we also observed enhanced sensitization effect of STAT3 inhibition on STING signaling in PMA-differentiated THP-1 macrophages (Supplementary Fig. S4).

Accumulating evidence indicates that cGAS-STING pathway is an important player in cancer immunity and is a potential therapeutic target for cancer treatment [23]. Tumor-derived DNA triggers the production of type I IFNs through the cGAS-STING pathway, which is essential for the maturation of DCs and priming of $CD8^+$ T cells that provide important

immunosurveillance against tumor cells. Intratumorial administration of STING agonists, including cGAMP and its modified analogues, effectively blocks tumor growth in mouse models of various malignancies [19, 33, 55]. c-diAM$(PS)_2$ (also known as ADU-S100 or MIW815) alone or in combination with immune checkpoint inhibitors are currently being evaluated in phase I clinical trials to treat advanced/metastatic solid tumors or lymphomas (NCT03172936, NCT03010176 and NCT02675439). On the other hand, the cGAS-STING pathway is associated with inflammation-driven carcinogenesis and immunosuppression, highlighting a necessity of fine tuning the cGAS-STING pathway in cancer immunotherapeutics [56]. Immunosuppression of the STING pathway may be attributable to increased regulatory T cell infiltration [57], MDSC infiltration [12], and induced immunoregulatory indoleamine 2,3-dioxygenase (IDO) enzyme [21]. Although detailed mechanisms for these observations warrant further characterization, feedback activation of STAT3 by the STING pathway may be the potential target involved in the observed tumor promoting effect and immunosuppressive activity of STING signaling, since STAT3 is a key molecular hub of tumorigenesis and tumor-mediated immune suppression [49, 50]. In this study, we observed that the STAT3 inhibitor HJC0152 synergizes with the STING agonist c-diAM$(PS)_2$ to decrease the infiltration of Tregs and MDSCs, and to increase the accumulation of cytotoxic $CD8^+$ T cells in the tumor microenvironment. In consistent with these observations, the combined HJC0152 and c-diAM(PS)2 treatment markedly upregulates the expression of cytokines such as CXCL10 and CXCL9 that are crucial for chemotaxis of $CD8^+$ T cells, as well as the expression of CD80 and CD86, costimulatory ligands of T cells (Fig. 5A, B). Moreover, the combined HJC0152 and c-diAM(PS)2 treatment also downregulates the expression of immune-suppressive genes such as TGFβ, S100A8 and S100A9 (Fig. 5A, B). Furthermore, the combination of HJC0152 and c-diAM$(PS)_2$ resulted in significant and lasting

inhibition of tumor growth in the 4T1 syngeneic mouse model, suggesting that the use of the STING agonist in conjunction with the STAT3 inhibitor is a promising strategy for cancer treatment. Given the more profound sensitization effect of STAT3 inhibition in cGAS$^{-/-}$ THP1 cells, we anticipate that the use of a combined STAT3 inhibitor and STING agonist treatment will be more effective in cGAS-defective cancer cell lines [58].

In summary, we here showed that STAT3 inhibition enhances STING signaling induced by a STING agonist, and that the STAT3 inhibitor HJC0152 synergizes with the STING agonist c-diAM(PS)$_2$ to induce anti-tumor immune responses in the tumor microenvironment. Our work provides a rationale for the combined use of STAT3 inhibitors and STING agonists in cancer immunotherapy.

Acknowledgements

This work was supported by funds from the NSFC (21521003, 81373326, and 21290183 to J.Q.; 81400826 to Q.L.), Shenzhen Science and Technology Innovation Program (JCYJ20150529095420031, JCYJ20170412150827191 to J.Q.; JCYJ20170818090609800 to Q.L.), program of the Science and Technology Committee of Guangdong (2014A030312004 and 2015A030313887 to Q.L.), and Adlai Nortye Biopharma Co., Ltd. We thank Dr. Zhengfan Jiang (Peking University, Beijing, China) for providing STING$^{-/-}$ THP1 cells.

Appendix A. Supplementary data

Supplementary data related to this article can be found at xxx

Conflicts of interest

No potential conflicts of interest were disclosed.

References

[1] H. Ishikawa, G.N. Barber, STING is an endoplasmic reticulum adaptor that facilitates innate immune signalling, Nature, 455 (2008) 674-678.

[2] W. Sun, Y. Li, L. Chen, H. Chen, F. You, X. Zhou, Y. Zhou, Z. Zhai, D. Chen, Z. Jiang, ERIS, an endoplasmic reticulum IFN stimulator, activates innate immune signaling through dimerization, Proc Natl Acad Sci, 106 (2009) 8653-8658.

[3] B. Zhong, Y. Yang, S. Li, Y.Y. Wang, Y. Li, F. Diao, C. Lei, X. He, L. Zhang, P. Tien, H.B. Shu, The adaptor protein MITA links virus-sensing receptors to IRF3 transcription factor activation, Immunity, 29 (2008) 538-550.

[4] L. Jin, P.M. Waterman, K.R. Jonscher, C.M. Short, N.A. Reisdorph, J.C. Cambier, MPYS, a novel membrane tetraspanner, is associated with major histocompatibility complex class II and mediates transduction of apoptotic signals, Mol. Cell. Biol., 28 (2008) 5014-5026.

[5] L. Sun, J. Wu, F. Du, X. Chen, Z.J. Chen, Cyclic GMP-AMP synthase is a cytosolic DNA sensor that activates the type I interferon pathway, Science, 339 (2013) 786-791.

[6] E.J. Diner, D.L. Burdette, S.C. Wilson, K.M. Monroe, C.A. Kellenberger, M. Hyodo, Y. Hayakawa, M.C. Hammond, R.E. Vance, The Innate Immune DNA Sensor cGAS Produces a Noncanonical Cyclic Dinucleotide that Activates Human STING, Cell Reports, 3 (2013) 1355-1361.

[7] J. Wu, L. Sun, X. Chen, F. Du, H. Shi, C. Chen, Z.J. Chen, Cyclic GMP-AMP is an endogenous second messenger in innate immune signaling by cytosolic DNA, Science, 339 (2013) 826-830.

[8] Y. Tanaka, Z.J. Chen, STING Specifies IRF3 phosphorylation by TBK1 in the Cytosolic DNA Signaling Pathway, Science Signaling, 5 (2012) ra20.

[9] W.M. Schneider, M.D. Chevillotte, C.M. Rice, Interferon-stimulated genes: a complex web of host defenses, Annu Rev Immunol, 32 (2014) 513-545.

[10] P.C. Heinrich, I. Behrmann, G. Muller-Newen, F. Schaper, L. Graeve, Interleukin-6-type cytokine signalling through the gp130/Jak/STAT pathway, Biochem. J., 334 (1998) 297-314.

[11] Y. Liu, A.A. Jesus, B. Marrero, D. Yang, S.E. Ramsey, G.A.M. Sanchez, K. Tenbrock, H. Wittkowski, O.Y. Jones, H.S. Kuehn, C.R. Lee, M.A. DiMattia, E.W. Cowen, B. Gonzalez, I. Palmer, J.J. DiGiovanna, A. Biancotto, H. Kim, W.L. Tsai, A.M. Trier, Y. Huang, D.L. Stone, S. Hill, H.J. Kim, C. St Hilaire, S. Gurprasad, N. Plass, D. Chapelle, I. Horkayne-Szakaly, D. Foell, A. Barysenka, F. Candotti, S.M. Holland, J.D. Hughes, H. Mehmet, A.C. Issekutz, M. Raffeld, J. McElwee, J.R. Fontana, C.P. Minniti, S. Moir, D.L. Kastner, M. Gadina, A.C. Steven, P.T. Wingfield, S.R. Brooks, S.D. Rosenzweig, T.A. Fleisher, Z. Deng, M. Boehm, A.S. Paller, R. Goldbach-Mansky, Activated STING in a vascular and pulmonary syndrome, N Engl J Med, 371 (2014) 507-518.

[12] H. Liang, L. Deng, Y. Hou, X. Meng, X. Huang, E. Rao, W. Zheng, H. Mauceri, M. Mack, M. Xu, Y.X. Fu, R.R. Weichselbaum, Host STING-dependent MDSC mobilization drives extrinsic radiation resistance, Nat Commun, 8 (2017) 1736.

[13] J. Ahn, H. Konno, G.N. Barber, Diverse roles of STING-dependent signaling on the development of cancer, Oncogene, 34 (2015) 5302-5308.

[14] S.R. Woo, M.B. Fuertes, L. Corrales, S. Spranger, M.J. Furdyna, M.Y. Leung, R. Duggan, Y. Wang, G.N. Barber, K.A. Fitzgerald, STING-Dependent Cytosolic DNA Sensing

Mediates Innate Immune Recognition of Immunogenic Tumors, Immunity, 41 (2014) 830-842.

[15] L. Deng, H. Liang, M. Xu, X. Yang, B. Burnette, A. Arina, X.D. Li, H. Mauceri, M. Beckett, T. Darga, X. Huang, T.F. Gajewski, Z.J. Chen, Y.X. Fu, R.R. Weichselbaum, STING-Dependent Cytosolic DNA Sensing Promotes Radiation-Induced Type I Interferon-Dependent Antitumor Immunity in Immunogenic Tumors, Immunity, 41 (2014) 843-852.

[16] Q. Zhu, S.M. Man, P. Gurung, Z. Liu, P. Vogel, M. Lamkanfi, T.D. Kanneganti, STING mediates protection against colorectal tumorigenesis by governing the magnitude of intestinal inflammation, Journal of Immunology, 193 (2014) 4779-4782.

[17] T. Ohkuri, A. Ghosh, A. Kosaka, J. Zhu, M. Ikeura, M. David, S.C. Watkins, S.N. Sarkar, H. Okada, STING contributes to antiglioma immunity via triggering type I IFN signals in the tumor microenvironment, Cancer Immunol Res, 2 (2014) 1199-1208.

[18] D. Chandra, W. Quispe-Tintaya, A. Jahangir, D. Asafu-Adjei, I. Ramos, H.O. Sintim, J. Zhou, Y. Hayakawa, D.K. Karaolis, C. Gravekamp, STING ligand c-di-GMP improves cancer vaccination against metastatic breast cancer, Cancer Immunol Res, 2 (2014) 901-910.

[19] L. Corrales, L.H. Glickman, S.M. McWhirter, D.B. Kanne, K.E. Sivick, G.E. Katibah, S.R. Woo, E. Lemmens, T. Banda, J.J. Leong, K. Metchette, T.W. Dubensky, Jr., T.F. Gajewski, Direct Activation of STING in the Tumor Microenvironment Leads to Potent and Systemic Tumor Regression and Immunity, Cell Rep, 11 (2015) 1018-1030.

[20] J. Ahn, T. Xia, H. Konno, K. Konno, P. Ruiz, G.N. Barber, Inflammation-driven carcinogenesis is mediated through STING, Nat Commun, 5 (2014) 5166.

[21] H. Lemos, E. Mohamed, L. Huang, R. Ou, G. Pacholczyk, A.S. Arbab, D. Munn, A.L. Mellor, STING Promotes the Growth of Tumors Characterized by Low Antigenicity via IDO Activation, Cancer Res, 76 (2016) 2076-2081.

[22] Q. Chen, A. Boire, X. Jin, M. Valiente, E.E. Er, A. Lopez-Soto, L. S. Jacob, R. Patwa, H. Shah, K. Xu, J.R. Cross, J. Massagué, Carcinoma–astrocyte gap junctions promote brain metastasis by cGAMP transfer, Nature, 533 (2016) 493.

[23] L. Corrales, S.M. McWhirter, T.W. Dubensky, Jr., T.F. Gajewski, The host STING pathway at the interface of cancer and immunity, J Clin Invest, 126 (2016) 2404-2411.

[24] W.-B. Wang, D.E. Levy, C.-K. Lee, STAT3 Negatively Regulates Type I IFN-Mediated Antiviral Response, The Journal of Immunology, 187 (2011) 2578.

[25] H.H. Ho, L.B. Ivashkiv, Role of STAT3 in type I interferon responses. Negative regulation of STAT1-dependent inflammatory gene activation, J Biol Chem, 281 (2006) 14111-14118.

[26] H. Yu, D. Pardoll, R. Jove, STATs in cancer inflammation and immunity: a leading role for STAT3, Nat. Rev. Cancer, 9 (2009) 798-809.

[27] H. Yu, R. Jove, The STATs of cancer--new molecular targets come of age, Nat. Rev. Cancer, 4 (2004) 97-105.

[28] T. Wang, G. Niu, M. Kortylewski, L. Burdelya, K. Shain, S. Zhang, R. Bhattacharya, D. Gabrilovich, R. Heller, D. Coppola, W. Dalton, R. Jove, D. Pardoll, H. Yu, Regulation of the innate and adaptive immune responses by Stat-3 signaling in tumor cells, Nat Med, 10 (2004) 48-54.

[29] M. Kortylewski, M. Kujawski, T. Wang, S. Wei, S. Zhang, S. Pilon-Thomas, G. Niu, H. Kay, J. Mule, W.G. Kerr, R. Jove, D. Pardoll, H. Yu, Inhibiting Stat3 signaling in the

hematopoietic system elicits multicomponent antitumor immunity, Nat Med, 11 (2005) 1314-1321.

[30] I. Kinjyo, H. Inoue, S. Hamano, S. Fukuyama, T. Yoshimura, K. Koga, H. Takaki, K. Himeno, G. Takaesu, T. Kobayashi, A. Yoshimura, Loss of SOCS3 in T helper cells resulted in reduced immune responses and hyperproduction of interleukin 10 and transforming growth factor-beta 1, J. Exp. Med., 203 (2006) 1021-1031.

[31] H.J. Chen, Z.D. Yang, C.Y. Ding, L.L. Chu, Y.S. Zhang, K. Terry, H.L. Liu, Q. Shen, J. Zhou, Discovery of O-Alkylamino-Tethered Niclosamide Derivatives as Potent and Orally Bioavailable Anticancer Agents, Acs Medicinal Chemistry Letters, 4 (2013) 180-185.

[32] Y. Wang, S. Wang, Y. Wu, Y. Ren, Z. Li, X. Yao, C. Zhang, N. Ye, C. Jing, J. Dong, Suppression of the Growth and Invasion of Human Head and Neck Squamous Cell Carcinomas via Regulating STAT3 Signaling and miR-21/β-catenin Axis with HJC0152, Molecular Cancer Therapeutics, 16 (2017) 578-590.

[33] J. Fu, D.B. Kanne, M. Leong, L.H. Glickman, S.M. McWhirter, E. Lemmens, K. Mechette, J.J. Leong, P. Lauer, W. Liu, K.E. Sivick, Q. Zeng, K.C. Soares, L. Zheng, D.A. Portnoy, J.J. Woodward, D.M. Pardoll, T.W. Dubensky, Jr., Y. Kim, STING agonist formulated cancer vaccines can cure established tumors resistant to PD-1 blockade, Sci Transl Med, 7 (2015) 283ra252.

[34] H. Ishikawa, Z. Ma, G.N. Barber, STING regulates intracellular DNA-mediated, type I interferon-dependent innate immunity, Nature, 461 (2009) 788-792.

[35] H. Konno, K. Konno, G.N. Barber, Cyclic dinucleotides trigger ULK1 (ATG1) phosphorylation of STING to prevent sustained innate immune signaling, Cell, 155 (2013) 688-698.

[36] T. Prabakaran, C. Bodda, C. Krapp, B.C. Zhang, M.H. Christensen, C. Sun, L. Reinert, Y. Cai, S.B. Jensen, M.K. Skouboe, J.R. Nyengaard, C.B. Thompson, R.J. Lebbink, G.C. Sen, G. van Loo, R. Nielsen, M. Komatsu, L.N. Nejsum, M.R. Jakobsen, M. Gyrd-Hansen, S.R. Paludan, Attenuation of cGAS-STING signaling is mediated by a p62/SQSTM1-dependent autophagy pathway activated by TBK1, EMBO J, 37 (2018).

[37] W.W. Luo, S. Li, C. Li, H. Lian, Q. Yang, B. Zhong, H.B. Shu, iRhom2 is essential for innate immunity to DNA viruses by mediating trafficking and stability of the adaptor STING, Nat Immunol, 17 (2016) 1057-1066.

[38] T. Saitoh, N. Fujita, T. Hayashi, K. Takahara, T. Satoh, H. Lee, K. Matsunaga, S. Kageyama, H. Omori, T. Noda, N. Yamamoto, T. Kawai, K. Ishii, O. Takeuchi, T. Yoshimori, S. Akira, Atg9a controls dsDNA-driven dynamic translocation of STING and the innate immune response, Proc Natl Acad Sci, 106 (2009) 20842-20846.

[39] V.K. Gonugunta, T. Sakai, V. Pokatayev, K. Yang, J. Wu, N. Dobbs, N. Yan, Trafficking-Mediated STING Degradation Requires Sorting to Acidified Endolysosomes and Can Be Targeted to Enhance Anti-tumor Response, Cell Rep, 21 (2017) 3234-3242.

[40] N. Dobbs, N. Burnaevskiy, D.D. Chen, V.K. Gonugunta, N.M. Alto, N. Yan, STING Activation by Translocation from the ER Is Associated with Infection and Autoinflammatory Disease, Cell Host & Microbe, 18 (2015) 157-168.

[41] M.G. Kemp, L.A. Lindsey-Boltz, A. Sancar, UV Light Potentiates STING (Stimulator of Interferon Genes)-dependent Innate Immune Signaling through Deregulation of ULK1 (Unc51-like Kinase 1), J Biol Chem, 290 (2015) 12184-12194.

[42] H. Guo, R. Konig, M. Deng, M. Riess, J. Mo, L. Zhang, A. Petrucelli, S.M. Yoh, B. Barefoot, M. Samo, G.D. Sempowski, A. Zhang, A.M. Colberg-Poley, H. Feng, S.M.

Lemon, Y. Liu, Y. Zhang, H. Wen, Z. Zhang, B. Damania, L.C. Tsao, Q. Wang, L. Su, J.A. Duncan, S.K. Chanda, J.P. Ting, NLRX1 Sequesters STING to Negatively Regulate the Interferon Response, Thereby Facilitating the Replication of HIV-1 and DNA Viruses, Cell Host Microbe, 19 (2016) 515-528.

[43] J.F. Almine, C.A. O'Hare, G. Dunphy, I.R. Haga, R.J. Naik, A. Atrih, D.J. Connolly, J. Taylor, I.R. Kelsall, A.G. Bowie, P.M. Beard, L. Unterholzner, IFI16 and cGAS cooperate in the activation of STING during DNA sensing in human keratinocytes, Nat Commun, 8 (2017) 14392.

[44] Y. Chen, L. Wang, J. Jin, Y. Luan, C. Chen, Y. Li, H. Chu, X. Wang, G. Liao, Y. Yu, H. Teng, Y. Wang, W. Pan, L. Fang, L. Liao, Z. Jiang, X. Ge, B. Li, P. Wang, p38 inhibition provides anti-DNA virus immunity by regulation of USP21 phosphorylation and STING activation, J. Exp. Med., 214 (2017) 991-1010.

[45] S. Pensa, G. Regis, D. Boselli, F. Novelli, V. Poli, STAT1 and STAT3 in tumorigenesis: two sides of the same coin?, Landes Bioscience2009.

[46] L. Lu, F. Zhu, M. Zhang, Y. Li, A.C. Drennan, S. Kimpara, I. Rumball, C. Selzer, H. Cameron, A. Kellicut, A. Kelm, F. Wang, T.A. Waldmann, L. Rui, Gene regulation and suppression of type I interferon signaling by STAT3 in diffuse large B cell lymphoma, Proc Natl Acad Sci, 115 (2018) E498-E505.

[47] K.L. Jonsson, A. Laustsen, C. Krapp, K.A. Skipper, K. Thavachelvam, D. Hotter, J.H. Egedal, M. Kjolby, P. Mohammadi, T. Prabakaran, L.K. Sorensen, C. Sun, S.B. Jensen, C.K. Holm, R.J. Lebbink, M. Johannsen, M. Nyegaard, J.G. Mikkelsen, F. Kirchhoff, S.R. Paludan, M.R. Jakobsen, IFI16 is required for DNA sensing in human macrophages by promoting production and function of cGAMP, Nat Commun, 8 (2017) 14391.

[48] L. Zhang, J. Mo, K.V. Swanson, H. Wen, A. Petrucelli, S.M. Gregory, Z. Zhang, M. Schneider, Y. Jiang, K.A. Fitzgerald, S. Ouyang, Z.J. Liu, B. Damania, H.B. Shu, J.A. Duncan, J.P. Ting, NLRC3, a member of the NLR family of proteins, is a negative regulator of innate immune signaling induced by the DNA sensor STING, Immunity, 40 (2014) 329-341.

[49] E.J. Hillmer, H. Zhang, H.S. Li, S.S. Watowich, STAT3 signaling in immunity, Cytokine Growth Factor Rev, 31 (2016) 1-15.

[50] H. Yu, M. Kortylewski, D. Pardoll, Crosstalk between cancer and immune cells: role of STAT3 in the tumour microenvironment, Nat Rev Immunol, 7 (2007) 41-51.

[51] Q. Chen, L. Sun, Z.J. Chen, Regulation and function of the cGAS-STING pathway of cytosolic DNA sensing, Nat Immunol, 17 (2016) 1142-1149.

[52] X. Zhou, Z. Jiang, STING-mediated DNA sensing in cancer immunotherapy, Sci China Life Sci, 60 (2017) 563-574.

[53] Wang, Qiang, Liu, Xing, Cui, Ye, Tang, Yijun, Chen, Wei, The E3 ubiquitin ligase AMFR and INSIG1 bridge the activation of TBK1 kinase by modifying the adaptor STING, Immunity, 41 (2014) 919-933.

[54] K. Hansen, T. Prabakaran, A. Laustsen, S.E. Jørgensen, S.H. Rahbæk, S.B. Jensen, R. Nielsen, J.H. Leber, T. Decker, K.A. Horan, Listeria monocytogenes induces IFNβ expression through an IFI16-, cGAS- and STING-dependent pathway, Embo Journal, 33 (2014) 1654.

[55] O. Demaria, A. De Gassart, S. Coso, N. Gestermann, J. Di Domizio, L. Flatz, O. Gaide, O. Michielin, P. Hwu, T.V. Petrova, F. Martinon, R.L. Modlin, D.E. Speiser, M. Gilliet,

STING activation of tumor endothelial cells initiates spontaneous and therapeutic antitumor immunity, Proc Natl Acad Sci, 112 (2015) 15408-15413.

[56] K.W. Ng, E.A. Marshall, J.C. Bell, W.L. Lam, cGAS-STING and Cancer: Dichotomous Roles in Tumor Immunity and Development, Trends Immunol, 39 (2018) 44-54.

[57] D. Liang, H. Xiao-Feng, D. Guan-Jun, H. Er-Ling, C. Sheng, W. Ting-Ting, H. Qin-Gang, N. Yan-Hong, H. Ya-Yi, Activated STING enhances Tregs infiltration in the HPV-related carcinogenesis of tongue squamous cells via the c-jun/CCL22 signal, Biochim Biophys Acta, 1852 (2015) 2494-2503.

[58] T. Xia, H. Konno, J. Ahn, G.N. Barber, Deregulation of STING Signaling in Colorectal Carcinoma Constrains DNA Damage Responses and Correlates With Tumorigenesis, Cell Reports, 14 (2016) 282.

Fig. 1. STAT3 inhibition enhances CDN-induced type I IFN signalling. (**A, B**) THP1 cells were treated with increasing amounts of HJC0152 (0, 5, 10 or 15 μM) in the presence or absence of 2 μg/ml c-diAM(PS)$_2$ for 8 hr. The mRNA expression levels of IFNβ (**A**) and CXCL10 (**B**) were assessed by real-time PCR and normalized to GAPDH expression. (**C, D**) THP1 cells were stimulated with 15 μM HJC0152 and 2 μg/ml c-diAM(PS)$_2$ as indicated. The samples were collected at the indicated times, and the mRNA expression levels of IFNβ (**C**) and CXCL10 **(D**) were compared. (**E, F**) THP1 cells were treated with increasing doses of c-diAM(PS)$_2$ (0, 0.5, 1 or 2 μg/ml) in the presence or absence of 15 μM HJC0152. At 48 hr after stimulation, IFNβ (**E**) and CXCL10 (**F**) protein levels in the supernatants were measured by ELISA. Error bars represent s.d. of independent experiments (n=3). ns, not significant, * $p < 0.05$, ** $p < 0.01$, *** $p < 0.001$ (Student's t-test).

Fig. 2. Loss of STAT3 enhances the activation of the cGAS-STING pathway by CDN. (**A**) THP1 cells were treated with 15 μM HJC0152 and 2 μg/ml c-diAM(PS)$_2$ as shown for the indicated times. Whole cell lysates were prepared, and the levels of total STAT3, phospho-STAT3 (pSTAT3-Tyr705), total TBK1, phospho-TBK1 (pTBK1-Ser172), total IRF3, phospho-IRF3 (pIRF3-Ser386), and GAPDH were assessed by western blotting. (**B**-**D**) THP1 cells were transfected with negative control siRNA (N.C.) or siRNA targeting STAT3 (siRNA A and B) for 36 hr and then were treated with 2 μg/ml c-diAM(PS)$_2$ for the indicated times. The mRNA expression levels of IFNβ and CXCL10 were assessed by real-time PCR and normalized to GAPDH expression (**B**, **C**). Error bars represent s.d. of independent experiments (n=3). * $p < 0.05$, ** $p < 0.01$, *** $p < 0.001$ (Student's t-test). Whole cell lysates were prepared, and the

levels of total STAT3, total IRF3, phospho-IRF3 (pIRF3-Ser386), GAPDH were assessed by immunoblotting (**D**).

Fig. 3. STAT3 inhibition enhances the cGAS-STING signalling in a STING-dependent manner. (**A, B**) THP1 cells, STING$^{-/-}$ THP1 cells and cGAS$^{-/-}$ THP1 cells were treated with 15 μM HJC0152 and 2 μg/ml c-diAM(PS)$_2$ as indicated for 12 hr. The mRNA expression levels of IFNβand CXCL10 were assessed and normalized to GAPDH expression (**A**, **B**). (**C**) Whole cell lysates were prepared, and the levels of total STAT3, phospho-STAT3 (pSTAT3-Tyr705), total TBK1, phospho-TBK1 (pTBK1-Ser172), total IRF3, phospho-IRF3 (pIRF3-Ser386), STING and GAPDH were assessed by immunoblotting. (**D**) STING$^{-/-}$ THP1 cells and cGAS$^{-/-}$ THP1 cells were stimulated with increasing amounts of c-diAM(PS)$_2$ in the presence or absence of 15 μM HJC0152 for 48 hr. IFNβ and CXCL10 protein levels in the supernatants were measured by ELISA. Error bars represent s.d. of independent experiments (n=3). * $p < 0.05$, ** $p < 0.01$, *** $p < 0.001$ (Student's t-test).

Fig. 4. STAT3 inhibition promotes STING translocation. THP1 cells were differentiated by 320 nM PMA for 30 h and then treated with 15 μM HJC0152 and 2 μg/ml c-diAM(PS)$_2$ individually or in combination for 30 minutes or 3 h. After that, the cells were fixed and co-stained with STING and an ERGIC marker (ERGIC/p58). (**A**) Fluorescent micrographs show STING/ERGIC localization in PMA-THP1 cells after treatment. Scale bar, 5 μm. (**B**) Quantitation of colocalization was calculated as Pearson's correlation coefficient (r) (n=10). * $p < 0.05$, ** $p < 0.01$, *** $p < 0.001$ (Student's t-test).

Fig. 5. STAT3 transcriptionally regulates STING signalling. (**A**) THP1 cells were stimulated

with 15 μM HJC0152 (H) or 2 μg/ml c-diAM(PS)$_2$ (C) or their combination (HC) for 12 hr. The total RNA was extracted and differentially expressed genes were analysed using the algorithm DEGseq. (**B**) Total gene expression (number of reads normalized to total reads) are presented for the 7 red-marked genes: IFNB1, CXCL10, CD80, S100A8, IFI16, INSIG1 and NLRC3. Error bars represent s.d. of samples (n=3). * $p < 0.05$, ** $p < 0.01$, *** $p < 0.001$ (Student's t-test).

Fig. 6. STAT3 inhibition enhances STING agonist-mediated anti-tumor response. (**A**) Mice with 4T1 tumors were injected i.t. with vehicle (n=6), HJC0152 (30 μg, n=6), c-diAM(PS)$_2$ (10 μg, n=6) or their combination (n=6) three times (indicated by arrows). The tumor volumes were measured at the indicated time points. (**B**) Mice were weighted at the indicated time points. In addition, the percent change in body weight from the baseline for each treatment was calculated. (**C**) The individual tumor volumes for each treatment at the indicated time points are presented. (**D, E**) Gross appearance (**D**) and weight (**E**) of the tumors extracted from tumor-bearing mice at day 27 after treatment initiation. Error bars represent s.d.. * $p < 0.05$, ** $p < 0.01$, *** $p < 0.001$ (Student's t-test). Scale bar, 1 cm.

Fig. 7. STAT3 inhibition enhances STING agonist-mediated anti-tumor immunity. (**A, B**) Tissue sections from 4T1 tumors receiving the indicated treatments were stained with an antibody for CD8a to detect cytotoxic T cells (**A**) or with Ly6G to detect MDSCs (**B**). The presented images are from representative sections of tumors. (**C**) The percentages of $CD3e^+$, $CD4^+$, $Foxp3^+$, $CD8^+$ and $Ly6G^+$ cells in the tumor sections were calculated individually from 6 images of different tumors from each treatment group. Error bars represent s.d. ns, not significant, * $p < 0.05$, ** $p < 0.01$, *** $p < 0.001$ (Student's t-test). Scale bar, 50 μm.

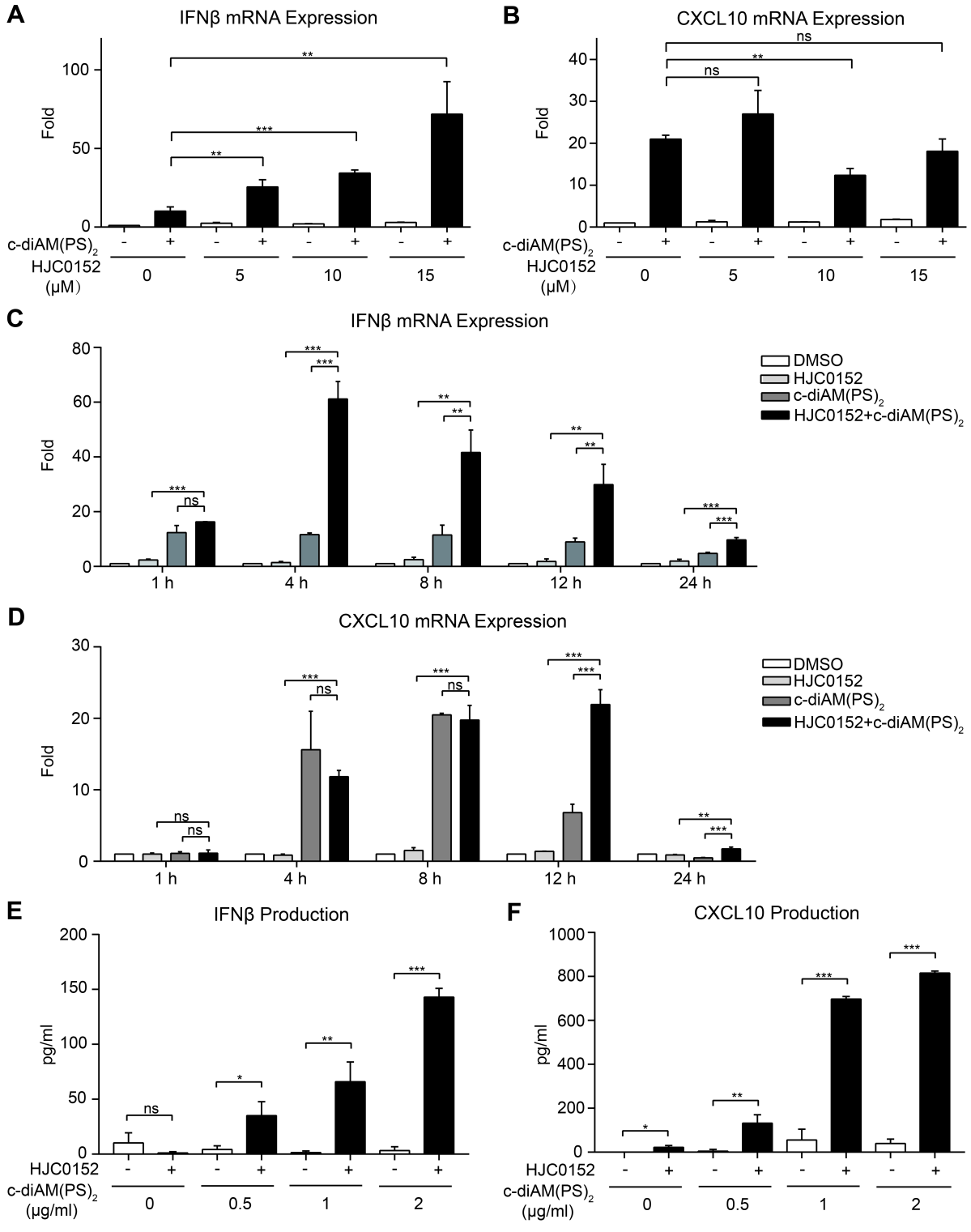
A
IFNβ mRNA Expression
Fold
c-diAM(PS)2
HJC0152
(μM)
B
CXCL10 mRNA Expression
C
IFNβ mRNA Expression
DMSO
HJC0152
c-diAM(PS)2
HJC0152+c-diAM(PS)2
1 h
4 h
8 h
12 h
24 h
D
CXCL10 mRNA Expression
E
IFNβ Production
pg/ml
c-diAM(PS)2
(μg/ml)
F
CXCL10 Production

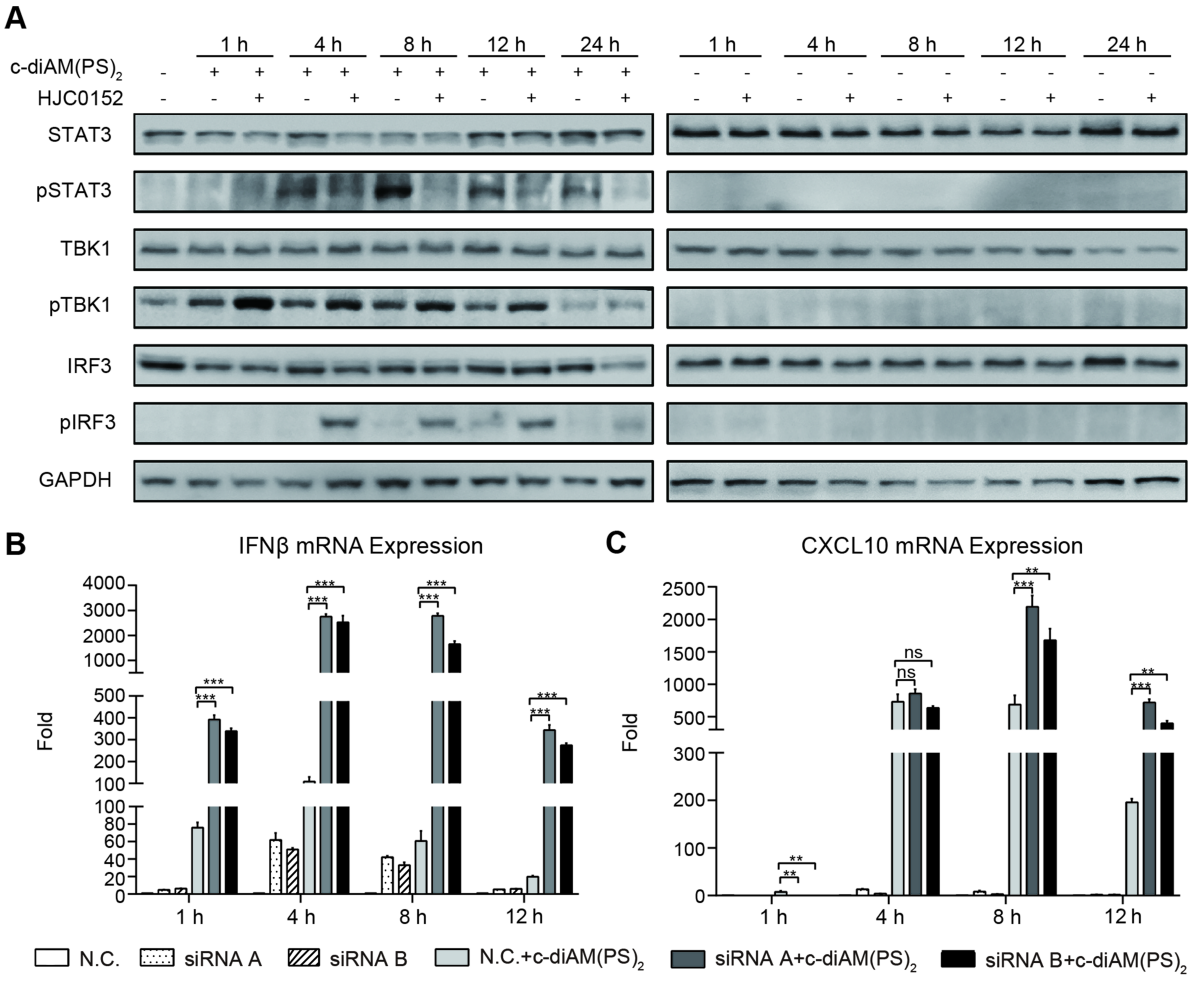
A
1 h
4 h
8 h
12 h
24 h
c-diAM(PS)2
HJC0152
STAT3
pSTAT3
TBK1
pTBK1
IRF3
pIRF3
GAPDH
B
IFNβ mRNA Expression
Fold
C
CXCL10 mRNA Expression
ns
N.C.
siRNA A
siRNA B
N.C.+c-diAM(PS)2
siRNA A+c-diAM(PS)2
siRNA B+c-diAM(PS)2
D
siRNA
NC
A
B

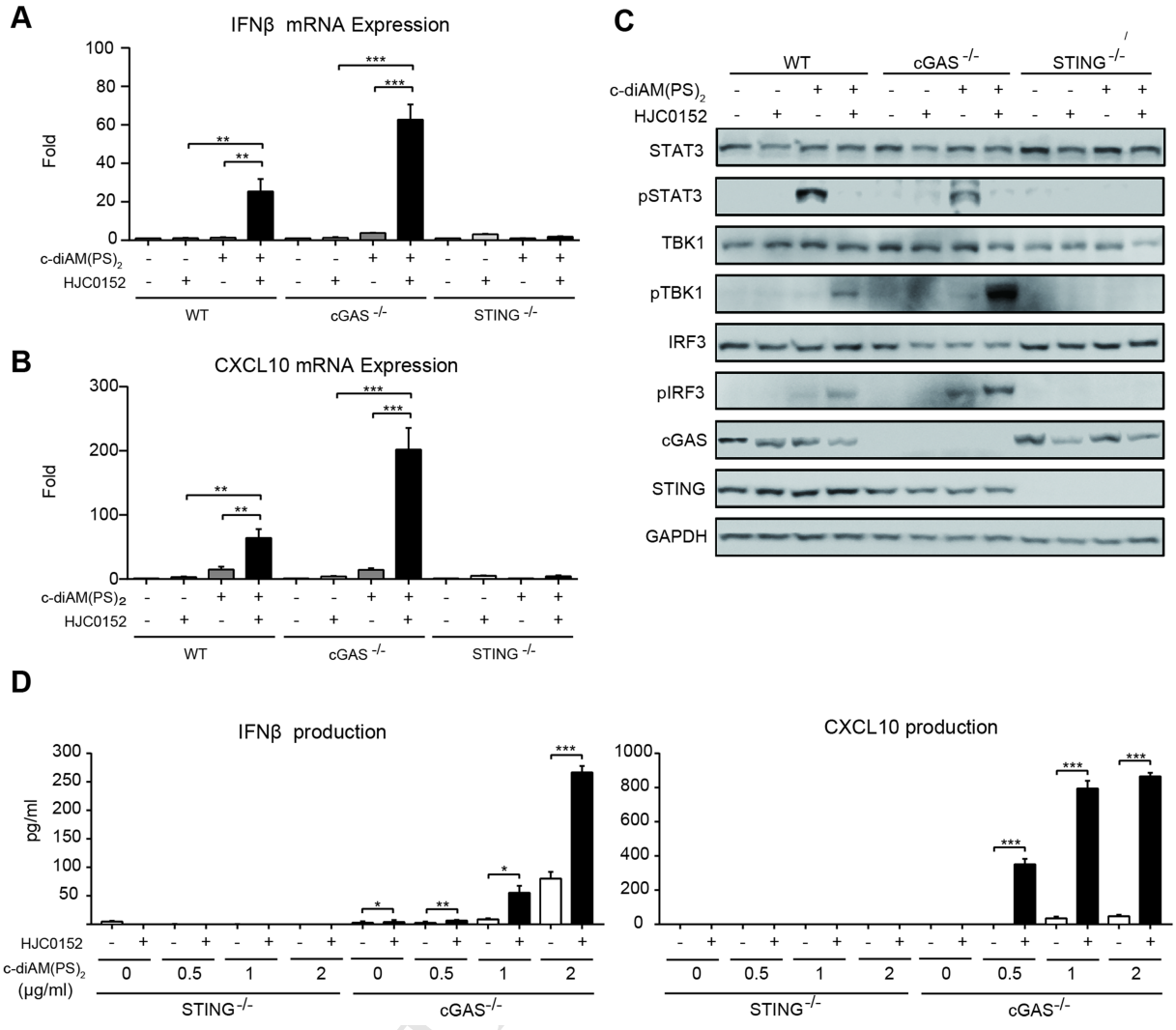
A
IFNβ mRNA Expression
Fold
c-diAM(PS)2
HJC0152
WT
cGAS -/-
STING -/-
B
CXCL10 mRNA Expression
C
STAT3
pSTAT3
TBK1
pTBK1
IRF3
pIRF3
cGAS
STING
GAPDH
D
IFNβ production
pg/ml
CXCL10 production
c-diAM(PS)2 (μg/ml)
STING-/-
cGAS-/-

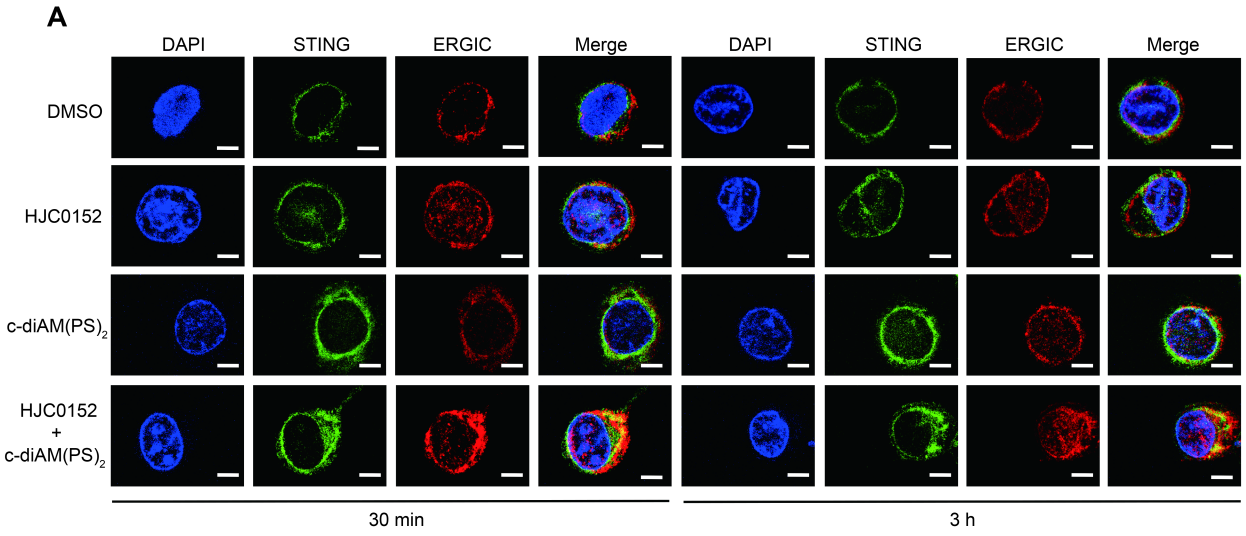

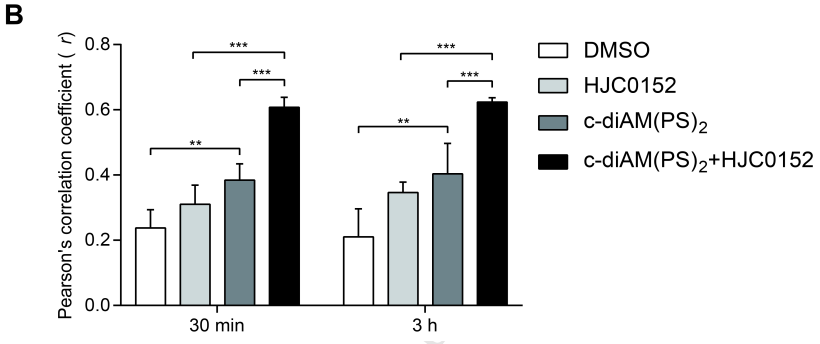

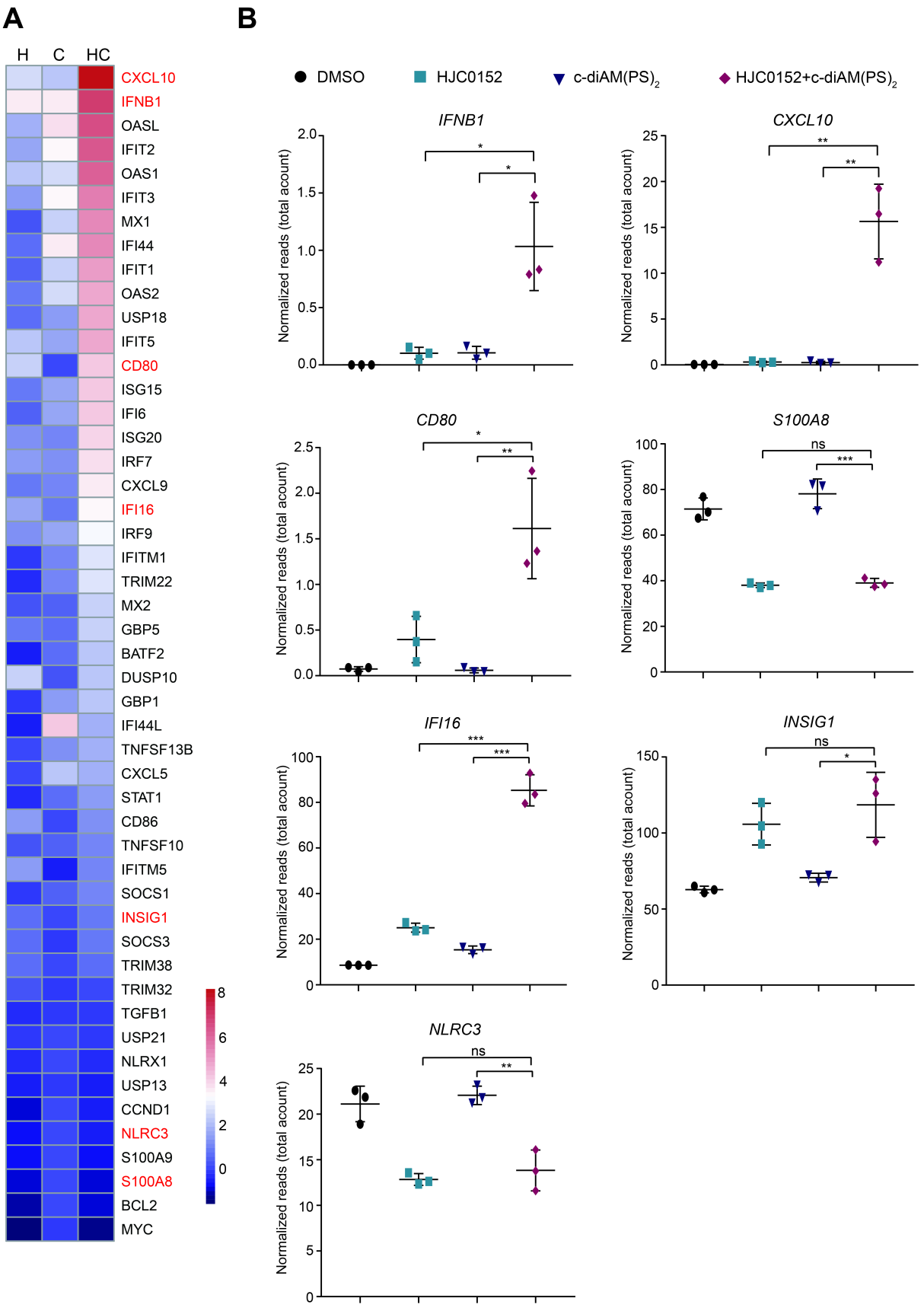
A
H
C
HC
CXCL10
IFNB1
OASL
IFIT2
OAS1
IFIT3
MX1
IFI44
IFIT1
OAS2
USP18
IFIT5
CD80
ISG15
IFI6
ISG20
IRF7
CXCL9
IFI16
IRF9
IFITM1
TRIM22
MX2
GBP5
BATF2
DUSP10
GBP1
IFI44L
TNFSF13B
CXCL5
STAT1
CD86
TNFSF10
IFITM5
SOCS1
INSIG1
SOCS3
TRIM38
TRIM32
TGFB1
USP21
NLRX1
USP13
CCND1
NLRC3
S100A9
S100A8
BCL2
MYC
8
6
4
2
0
B
DMSO
HJC0152
c-diAM(PS)2
HJC0152+c-diAM(PS)2
IFNB1
CXCL10
CD80
S100A8
IFI16
INSIG1
NLRC3
Normalized reads (total acount)
ns

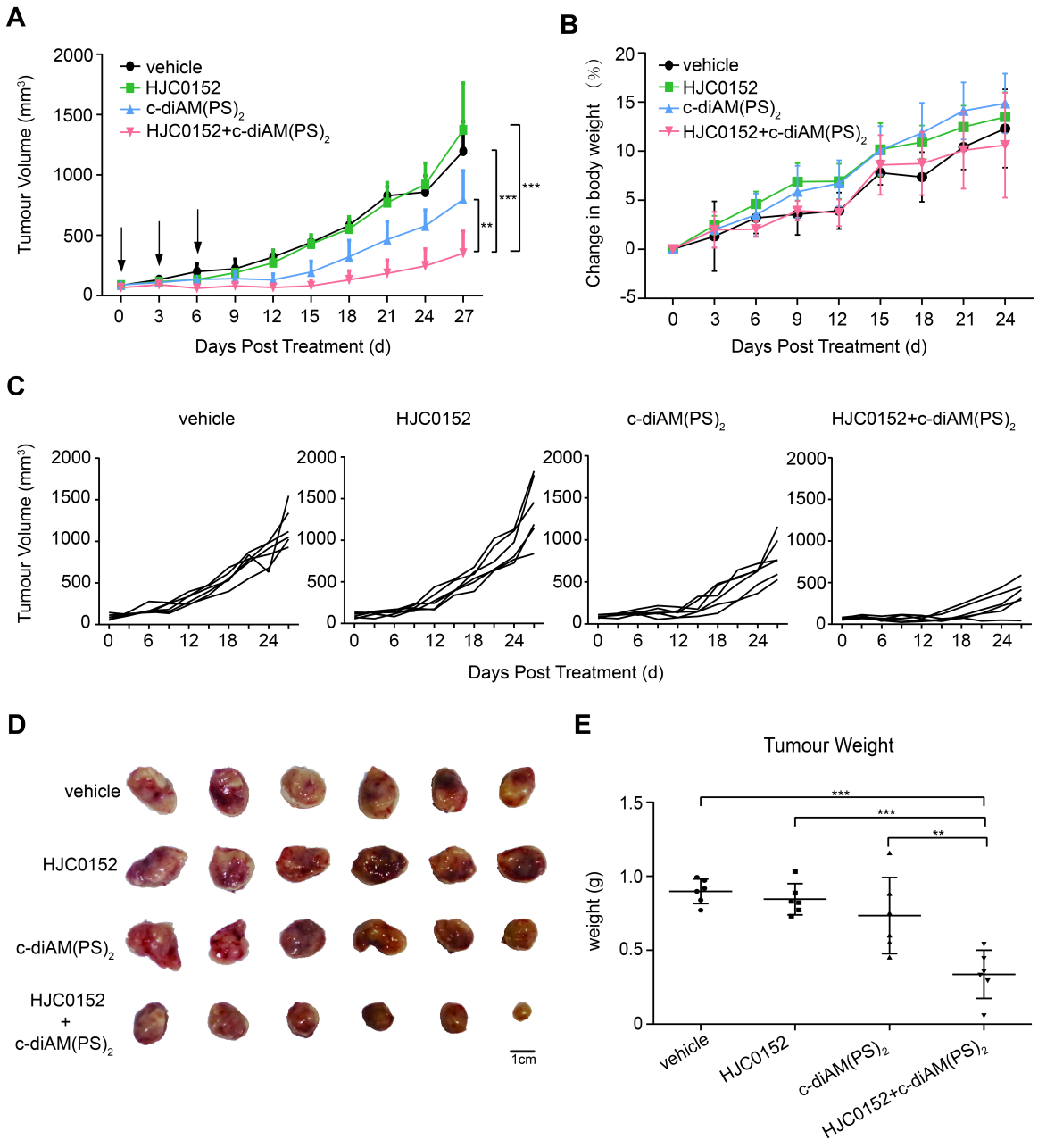
A
Tumour Volume (mm3)
vehicle
HJC0152
c-diAM(PS)2
HJC0152+c-diAM(PS)2
Days Post Treatment (d)
B
Change in body weight (%)
C
vehicle
HJC0152
c-diAM(PS)2
HJC0152+c-diAM(PS)2
D
1cm
E
Tumour Weight
weight (g)

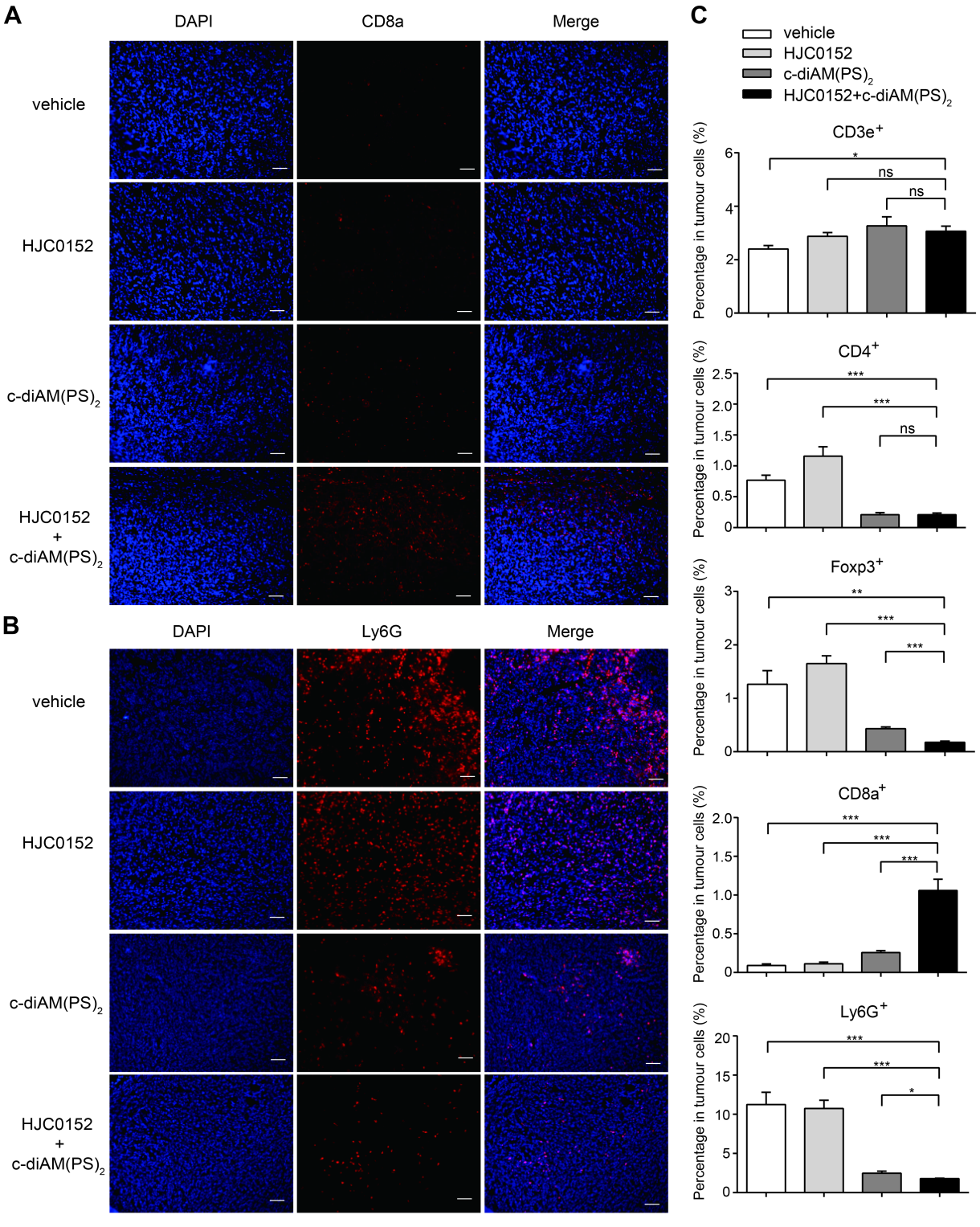
A
DAPI
CD8a
Merge
vehicle
HJC0152
c-diAM(PS)2
HJC0152 + c-diAM(PS)2
B
DAPI
Ly6G
Merge
vehicle
HJC0152
c-diAM(PS)2
HJC0152 + c-diAM(PS)2
C
vehicle
HJC0152
c-diAM(PS)2
HJC0152+c-diAM(PS)2
CD3e+
CD4+
Foxp3+
CD8a+
Ly6G+
Percentage in tumour cells (%)
ns
*
**
***

Highlights:

1. STAT3 inhibition enhances CDN-induced STING signaling.
2. The sensitization effect of STAT3 inhibition depends on STING rather than cGAS.
3. HJC0152 and c-diAM$(PS)_2$ synergize to inhibit tumor growth in vivo.
4. HJC0152 and c-diAM$(PS)_2$ synergize to induce antitumor immunity in the TME.

Jianwen Pei: Conceptualization, Methodology, Validation, Formal Analysis, Investigation, Resources, Data Curation, Writing, Visualization. **Yibo Zhang**: Conceptualization, Methodology, Validation, Formal Analysis, Investigation, Resources, Data Curation, Writing, Visualization. **Qinhong Luo**: Methodology, Validation, Formal Analysis, Investigation, Visualization, **Wenlv Zheng**: Methodology, Validation, Formal Analysis, Investigation. **Wanxuan Li**: Methodology, Validation, Formal Analysis, Investigation. **Xin Zeng**: Methodology, Validation, Formal Analysis, Investigation. **Qinkai Li**: Methodology, Validation, Formal Analysis, Investigation, Funding Acquisition. **Junmin Quan**: Conceptualization, Methodology, Validation, Formal Analysis, Investigation, Resources, Data Curation, Writing, Visualization, Supervision, Project Administration, Funding Acquisition.